Korean J. Chem. Eng., **23**(4), 560-565 (2006)

On the modeling of electro-hydrodynamic flow in a wire-plate electrostatic precipitator

Young Nam Chun† and Dong Seok Yeom*

Department of Environmental Engineering, Chosun University, Seosuk-dong, Gwangju 501-759, Korea
*ACT2000, 290-1, Geoyeo-dong, Seoul 138-110, Korea
(*Received 14 July 2005 • accepted 9 February 2006*)

Abstract–Modeling of the flow velocity fields for the electrohydrodynamic (EHD) flow in a wire-to-plate type electrostatic precipitator (ESP) was achieved. Solutions of the steady, two-dimensional Navier-Stokes equations have been computed. The equations were solved in the conservative finite-difference form on a fine uniform rectilinear grid of sufficient resolution to accurately capture the momentum boundary layers. The numerical procedure for differential equations was used by SIMPLEST [Michel, 2002], a derivative of Patankar's SIMPLE algorithm, to bring rapid convergence. The Phoenics (Version 3.5.1) CFD code, coupled with Poisson's and ion transport equations and electric body force in the momentum equation, developed in this study, was used for the numerical simulation. From calculations for the flow employing different flow models, the Chen-Kim $k-\varepsilon$ turbulent model appeared to be the most appropriate choice to obtain a quantitative image of the resulting mean flow field and downstream wake flow of the rear wire, although this was obtained from a qualitative analysis due to the lack of experimental verification. The flow velocity field pattern showed a strong EHD secondary flow, which was clearly visible in the downstream regions of the corona wire despite the low Reynolds number for the electrode (Re_{CW}=12.4). Secondary flow vortices were also caused by the EHD with increases in the discharge current.

Key words: EHD, ESP, Chen-Kim Model, Modeling, Von-Karman Vortex

INTRODUCTION

Industrial electrostatic precipitation has a very complex interaction mechanism that involves the electric field, and gas and particulate flows [Young et al., 2004]. The motion and precipitation of dust particles in an ESP depends on the electric field, space charge, gas flow field and dust particle properties. It has previously been shown [Yamamoto and Velkoff, 1981; Park and Park, 2005] that a significant interaction exists between the dust particle collections and EHD flow in ultra-fine particle precipitation processes.

However, it is still unclear whether these turbulent flow structures advance or deteriorate fine particle precipitation processes. The elucidation of the influence of electrically generated flow disturbances in a high resistivity cleaning process in intermediate spacing ESPs requires further investigation. EHD turbulence can be generated, even for Reynolds number less than 2.0, if the EHD number (Ehd) is larger than the square of the critical Reynolds number ($Ehd>Re^2$) [Chang et al., 2005], which is a common operation condition for commercial ESPs, so it is important to know the turbulent flow to improve the efficiency of fine particle collection.

Since Yamamoto and Velkoff [1981] first performed numerical calculations to solve the equations governing fluid flow and the electric field, for the investigation of the particle-free secondary flow interaction between those fields, turbulent EHD analyses have been carried out to calculate the EHD flow field by solving the time-averaged Navier-Stokes equations, using $k-\varepsilon$ turbulence closure [Choi and Fletcher, 1997], RNG $k-\varepsilon$ [Park and Kim, 2000] and Reynolds stress models [Schemid et al., 2002]. Although the above turbulence models have previously been successfully applied in a few cases, yielding what were assumed to be reasonable results for practical ESP conditions, discussions continue on the validity of these turbulence models for ESP applications due to the isotropic assumption and/or their difficulty in showing small eddy effects, as they only appear useful for models with a high Reynolds number. Therefore, another turbulent model, which can show more details, particularly for a small wake (e.g., Von-Karman vortex) at the near wire, is required.

The physical mechanism of EHD flow is based on a model where the ions produced by the corona are discharged near to the corona wire and move toward the grounded wall due to the Coulomb force. The ions provide a bulk body force to the fluid flow, resulting from the collision between the ions and neutral molecules. The body force causes the flow field to become complicated, as expressed by the product source of the space charge density and the electric field strength in the momentum equation [Liang and Lin, 1994].

Although there have been many experimental investigations on the particle transport in ESPs, so far only a few have directly accessed the flow field inside the precipitation zone. This is due to the complex electrical interactions: measuring techniques using probes will interfere with the electric field and are therefore inappropriate. Conversely, most non-intrusive optical techniques rely on the use of tracer particles, which are not solely influenced by the flow field, but by the electric field also; hence, only indirect information can be obtained, which is difficult to compare with model calculations.

In the present study, a turbulent low/high Reynolds number model was selected to show EHD flow, particularly the wake downstream near the wire. Furthermore, the physics and mechanisms of ionic wind formation were clarified by this selected Chen-Kim modified $k-\varepsilon$ turbulent model [Monson et al., 1990].

†To whom correspondence should be addressed.
E-mail: ynchun@chosun.ac.kr

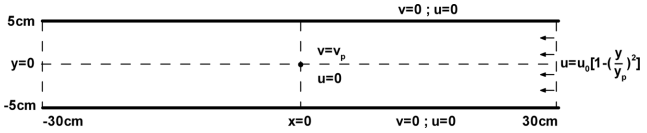

Fig. 1. Boundary conditions used in the present calculations.

NUMERICAL SIMULATION

1. General Simulation Procedure

Numerical studies were performed for a one wire-plate electrostatic precipitator. The corona discharge wire, 0.9 mm in diameter, was placed in the center of the horizontal parallel plate electrodes. The lengths of the plate electrodes were 60 cm, with a gap of 10 cm. Fig. 1 shows the ESP geometry and boundary conditions.

Steady-state two-dimensional fields were assumed to simplify the physical phenomena. The turbulent fluid flow within an ESP was calculated by using the commercially available Phoenics (Version 3.5.1) CFD code, with a finite volume method for the time-averaged Navier-Stokes equations closed by the k–ε turbulent model. A laminar model was also used to calculate the lamina flow without an EHD flow.

The electric field and ion charge density were obtained from calculations of the Poisson's (see Eq. (1)) and ion transport equations (see Eq. (2)), respectively, and achieved by using pseudo-methodology with equations derived for wire-pipe ESP [Chang et al., 1997].

The ion charge density, electric field and space charge terms of the momentum equations were programmed into the user defined subroutines of the Phoenics code. The governing equations for the EHD flow field (u_i, k, ε) and electric field (E_r, N_c) were solved by iterative solvers, which were cycled through the equation sequence of the global iteration for coupling between the equations.

Table 1 shows the conditions for finding the effects of various applied voltages and gas flow velocities. Cases E1-E5 are to know the effects of applied voltage at same gas flow velocity 0.2 m/s (Re_{CW}= 12.4 at corona wire, Re_{FC}=1,377 at flow channel). Case v0.8 is to show the effects of gas flow velocity change at same voltage (Ehd_{CW} =1.31×10^6, Ehd_{FC}=4.04×10^2) like Case E1.

2. Electric Field and space Charge Distribution

The strength of the electric field and the ion charge density were determined by using Poisson's (Eq. (1)) and the ion transport equations (Eq. (2)) for cylindrical coordinate [Chang et al., 1997].

$$\frac{1}{r}\frac{d(rE_r)}{dr} = -\frac{eN_c}{\varepsilon} \tag{1}$$

$$\frac{I_c}{2\pi rL} = e(U_{gr} + \mu_c E_r)N_c \tag{2}$$

Table 1. The effect of the conditions on the voltage

Case	Voltage (kV)	Current (μA)	Ehd_{CW}	Ehd_{FC}
E1	+19.9	20	1.31×10^6	4.04×10^2
E2	+22.2	30	1.96×10^6	6.06×10^2
E3	+24.1	40	2.61×10^6	8.08×10^2
E4	+25.1	60	3.92×10^6	1.21×10^3
E5	+29.1	90	5.88×10^6	1.82×10^3

where E_r is the electric field, r the radius, N_c the number of ions, e the electric elementary charge (=1.6021892×10^{-19} C), ε the dielectric constant (=8.85418782×10^{-12} F/m), I_c the current, L the plate depth, U_{gr} the mean gas velocity and μ_c the mobility (=0.0002546 cm^2/Vs).

By integrating Eq. (1), the strength of the electric field is expressed as:

$$E_r = \left(\frac{I_c}{2\pi\varepsilon\mu_c L} + \frac{c_0^2}{r^2}\right)^{0.5} \tag{3}$$

where c_0 is the integration constant calculated from the appropriate current-voltage relationship [Chang et al., 1996].

The number of ions in Eq. (4) is expressed by Eq. (2).

$$N_c = \frac{I_c}{e2\pi rL(U_{gr} + \mu_c E_r)} \tag{4}$$

Therefore, the ion charge density can be calculated from Eq. (5).

$$\rho_{ion} = eN_c \tag{5}$$

3. EHD Flow Field

For a steady-state incompressible turbulent flow, the continuity and momentum equations are written as:

$$\frac{\partial}{\partial x_i}(\rho u_i) = 0 \tag{6}$$

$$\frac{\partial}{\partial x_j}(\rho u_i u_j) = -\frac{\partial p}{\partial x_i} + \frac{\partial}{\partial x_j}\left[(\mu + \mu_t)\left(\frac{\partial u_i}{\partial x_j} + \frac{\partial u_j}{\partial x_i}\right) - \rho\overline{u_i' u_j'}\right] + \rho_{ion}E_i \tag{7}$$

where u is the fluid mean velocity, p the mean static pressure, μ_t the turbulent eddy viscosity, u′ the fluctuation velocity, ρ_{ion} the ion charge density and E_i the strength of the electric field. The electric field strength and ion charge density are calculated from Eqs. (3) and (5), respectively.

Using the Boussinesque eddy-viscosity hypothesis, the Reynolds stress tensor is expressed as:

$$-\rho\overline{u_i' u_j'} = \mu_t\left(\frac{\partial u_i}{\partial x_j} + \frac{\partial u_j}{\partial x_i}\right) - \rho k\frac{2}{3}\delta_{ij} \tag{8}$$

where δ_{ij} is the Kronecker delta.

The turbulent eddy viscosity is:

$$\mu_t = \rho C_\mu \frac{k^2}{\varepsilon} \tag{9}$$

so it is calculated from the solution of the conservation equations of the turbulent kinetic energy (k) and the turbulent dissipation rate (ε) in the standard k–ε model (hereafter referred to as KE) [Launder and Spalding, 1974].

The k–ε model employs a single time scale (k/ε) to characterize the various dynamic processes that occur in turbulent flows. Turbulence, however, is comprised of fluctuating motions, with a spectrum of time scales, and a single-scale approach is unlikely to be adequate under all circumstances, as different turbulence interactions are associated with different parts of the spectrum. In order to remedy this deficiency in the standard model, Chen and Kim [Monson et al., 1990] proposed a modification that improves the dynamic response of the ε equation. The Chen Kim modified k–ε turbulent model (referred to as CK) should be proposed as both low and high

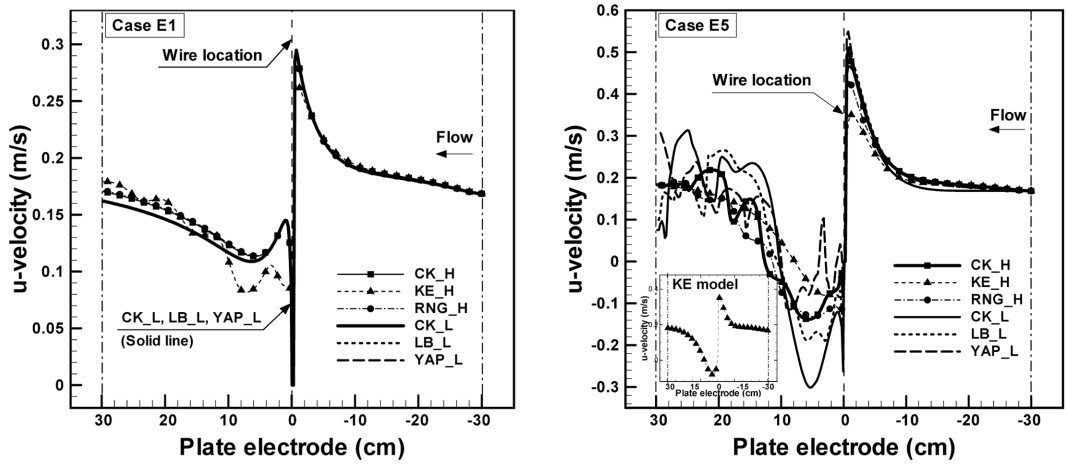

Fig. 2. Streamwise u-velocity with selected turbulent models.

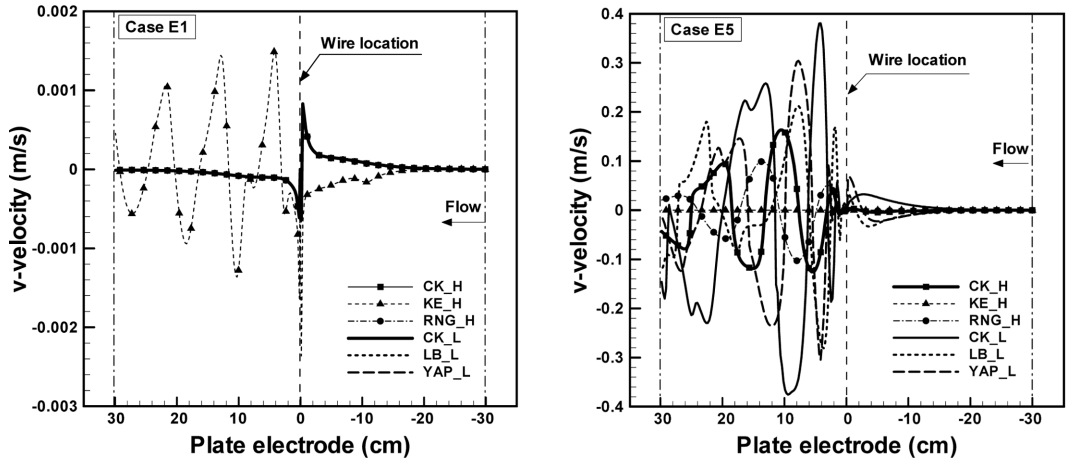

Fig. 3. Streamwise v-velocity with selected turbulent models.

Reynolds number models.

In addition, low Reynolds number models were used by Lam-Bremhorst low-Re extension to the $k-\varepsilon$ model (LB) [Patel et al., 1984], 'Yap' correction for separated flows (YAP) [Yap, 1987], and high Reynolds number models were used by RNG derived $k-\varepsilon$ turbulence model (RNG) [Yakhot and Orszag, 1986] to compare the different models.

The dimensionless EHD number and the Reynolds number at the plate and the wire were calculated by the definitions below [IEEE-DEIS-EHD Technical Committee, 2003].

The EHD numbers at the plate and wire are defined in Eq. (10).

$$Ehd_{CP}=\frac{I_0 L^3}{\rho_f \nu_f^2 \mu_i A} \text{ at the plate, } Ehd_{CW}=\frac{I_0 d^3}{\rho_f \nu_f^2 \mu_i A} \text{ at the wire} \qquad (10)$$

where, I_0 is the reference current, L the characteristic length, ρ_f the fluid density, ν_f the fluid kinematic viscosity, μ_i the mobility, A the surface area and d the wire diameter.

RESULTS AND DISCUSSION

1. Flow Modeling for EHD Flow

We have conducted many calculations on the numerous different turbulent models embedded within the Phoenics code, which are currently used for calculating turbulent flow. Of these, selected turbulent models are presented in Figs. 2 and 3 to show the characteristic of models and to propose a suitable model for EHD flow. Case E1 represents low turbulent flow formed when a low voltage is applied and Case E5 a high turbulent flow formed when a low voltage is applied.

Fig. 2 shows the u-velocity along the symmetry line through the corona wire, considering the u-velocity of the charged particle since the x-directional electric force is negligible on the symmetry line.

In the case of a low applied voltage (Case E1), the u-velocities for the so-called 'low Reynolds number models' were almost the same. However, for the high Reynolds number models those downstream were larger than with the low Reynolds number models, which were also different due to the different model characteristics. This means that high Reynolds number models will over-estimate for low voltages.

In the cases of a high applied voltage (Case E5), most turbulent models, with the exception of the $k-\varepsilon$ model, had fluctuations at downstream, while the low turbulent models (i.e., CK, LB and Yap models) had larger fluctuations. Larger fluctuations mean that larger irregular bulk motions should be fully developed in the ESP chan-

nels. The u-velocity of the $k-\varepsilon$ model shows an S shape, as can be seen in Fig. 2. This is because the standard $k-\varepsilon$ model could not express the small eddy effects, such as the EHD body force. However, the high Reynolds CK_H and RNG_H models are suitable for showing the appropriate wake of the downstream flow.

The wall-normal component v-velocity, as shown in Fig. 3, is an alternative quantity for describing the secondary flows. Since the statistical mean value of this component equals zero for a fully developed turbulent duct flow without volume forces, the v-velocities can be solely attributed to the ionic wind. This representation is particularly helpful for judging the influence of the secondary flows on the particle transport because this flow velocity component either promotes or hinders the particle transport.

In the case of a low applied voltage (Case E1), all the models, with the exception of the $k-\varepsilon$ model, had almost the same v-velocity. This is the reason why these models have the character which is possible to show the bulk body forces in the low turbulent flow. However, the standard $k-\varepsilon$ model had large irregular fluctuations, which may show that the model is not stable and does not converge well with a low turbulent flow.

In the case of a high applied voltage (Case E5), all turbulent models, with the exception of the $k-\varepsilon$ model, had fluctuations, while the low turbulent models showed larger fluctuations. As explained for Case E5 in Fig. 2, the high Reynolds CK modified $k-\varepsilon$ turbulent model can be adapted to show the appropriate wake for the rear flow of the wire. The v-velocity of the standard $k-\varepsilon$ model is zero, which represents no secondary flow in the center line.

Many experimental results [Riehle and Löffler, 1995] have confirmed that the corona induced-turbulence is at a significant level in conventional ESP. Particularly, turbulent EHD is more important at the near wire.

The turbulence model that accounts for the electrically induced turbulent flow remains to be established. Despite the limitation of the present turbulence model, not considering the electrically induced turbulence in the correction, the numerical prediction shows a qualitatively sufficient tendency when using the standard $k-\varepsilon$ models [Choi and Fletcher, 1997]. However, this model could not show the wake flow of the rear and near wire in detail, as it cannot show small scale effects. Although the Chen-Kim modified $k-\varepsilon$ turbulent model, which has low and high Reynolds models, was derived from qualitative analysis, it was most effective for turbulent EHD flow, as it can show small eddy effects of the bulk body, such as the Von-Karman vortex in the rear flow of the wire.

2. Influence of EHD Number

EHD computation was performed for electrical potentials of 19.9, 22.2, 24.1, 25.1 and 29.1 kV, while the primary flow velocity was maintained at 0.2 m/s (see Table 1). The results of the present computation can be applied to estimate the EHD for other electrical potentials as long as the EHD number [the so-called Ehd in Eq. (10)] is the same.

Fig. 4 shows the flow distribution for various applied voltages.

Without an applied voltage, 0 kV, for which the EHD numbers based on the corona wire and flow channel are $Ehd_{CW}=0$ and $Ehd_{FC}=0$, respectively, "Lamina" in Fig. 4 shows the usual lamina flow in the channel, as would be expected from Reynolds numbers of $Re_{CW}=12.4$ and $Re_{FC}=1{,}377$. However, once the EHD numbers increase from those used in Case E1 ($Ehd_{CW}=1.31\times10^6$) to those in

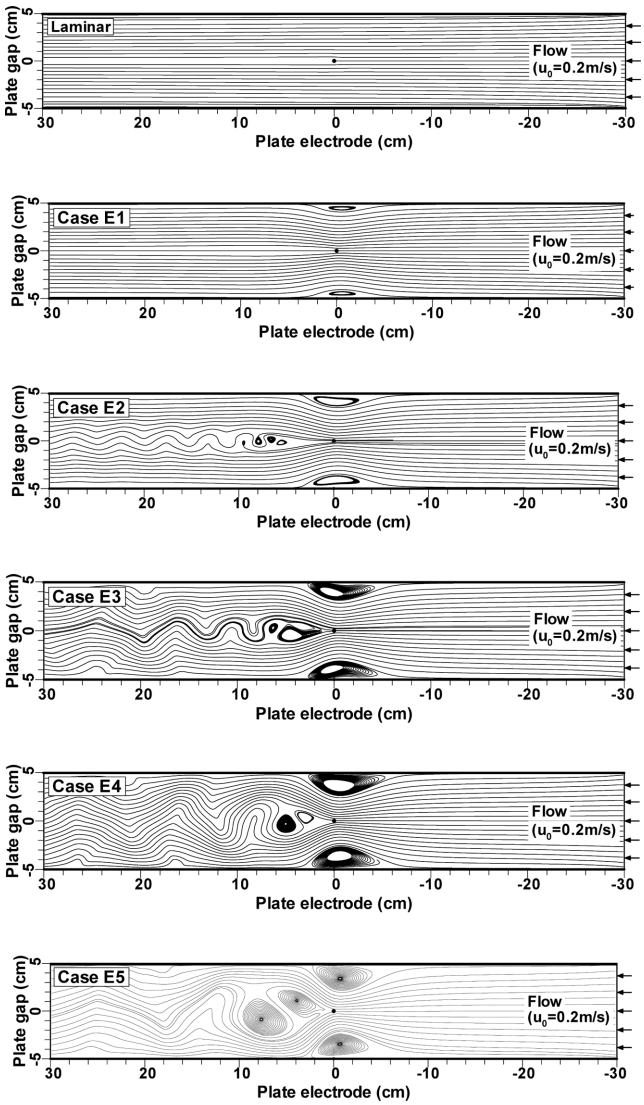

Fig. 4. Streamlines for various EHD numbers.

Case E5 ($Ehd_{CW}=5.88\times10^6$), not only were unsteady wakes observed, but some forward wakes were also evident. Particularly, the Von-Karman vortex stream was observed in Case E2 ($Ehd_{CW}=1.96\times10^6$), and with increases in the EHD number, such as in Case E3 ($Ehd_{CW}=2.61\times10^6$) through to Case E5, the downstream vortices in the channels were fully developed.

As the applied voltage increases, a greater amount of flow interaction takes place. At the applied voltage of 29.1 kV (Case E5), it was clear that the gas entering the channel gradually accelerated, being deflected towards the center line of the channel due to the secondary flow (i.e., ionic wind or electric wind). The level of this electrically generate turbulence was significant as there were strong interactions between the electric field, the electric charge and the gas flow. The investigation of the near-collection electrode region shows the importance of the secondary vortex flow. This means that secondary flows can have a great impact on the motion and precipitation of small particles, mainly those in the submicron range [Mizeraczyk et al., 2001].

Fig. 5 shows streamwise velocity profiles along the symmetry

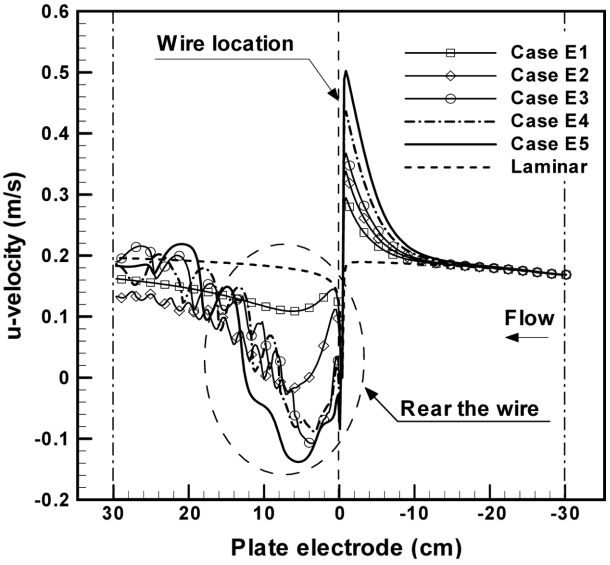

Fig. 5. Streamwise velocities for different Ehds.

line, via the corona wire, with no applied voltage and with different applied voltages for the flow velocity, u_0=0.2 m/s.

When no voltage ("Laminar" in Fig. 5) was applied to the wire electrode, the velocity was only slightly changed at the outlet. However, the character of the flow changed dramatically after a voltage was applied, with the flow becoming turbulent and showing many different turbulent structures, as explained in Fig. 4.

The gas velocity near the corona wire increased close to the front of the wire, but drastically decreased at the rear of the wire as the applied voltage was increased. This was caused by the corona wind induced by the electric body force of ions. The increasing velocity at the front wire is due to the increase in the counter flow to compensate for the vertical bulk flow, which travels in the direction of the plate electrode from the wire. Otherwise, the decrease at the rear wire is due to the streamwise velocity being decreased by the reversed counter flow. Particularly, in the case of applied high voltages (Cases E3 to E5), the velocities had negative values and fluctuated due to the large flow turbulence.

Those occur because the reversed counter flow was increased more gradually by the increase in the EHD number; i.e., an increase in the applied voltage.

SUMMARY AND CONCLUSIONS

The numerical simulation was achieved by using Phoenics (Version 3.5.1) CFD code, coupled with the Poisson's and ion transport equations (Eqs. (3) and (4)) and the electric body force of the momentum equation in Eq. (7), which was developed in this study.

To adapt a suitable model for EHD turbulent flow, comparisons were achieved for low and high turbulent flow models, which are known to have particularly good characteristics for small-scale effects.

With the use of flow calculations with different flow models, the Chen-Kim modified $k-\varepsilon$ turbulent model revealed similar structures for the secondary flows, which were shown particularly well for Von-Karman vortex and for the volume force-velocity fluctuation correlations in the ESP. Therefore, the CK model seems to be an appropriate choice for obtaining a quantitative image of the resulting mean flow field, although it had to be derived from qualitative analysis due to the lack of experimental verification.

The numerical results of the selected CK model are as follows:

1. The flow interaction took place when a voltage was applied. The inflow gas was gradually accelerated, and then deflected towards the center line of the channel due to the secondary flow produced by increasing the applied voltage.

2. Once EHD numbers were increased, not only were wakes observed, but some forward wakes were also evident. Particularly, the so-called Von-Karman vortex stream was observed at Ehd_{CW}=1.96×10^6. Also with the increase in the EHD number, as with Ehd_{CW}= 2.61×10^6, 3.92×10^6 and 5.88×10^6, the vortices in the rear flow channel were fully developed.

ACKNOWLEDGMENTS

This study was supported by research funds from Chosun University, 2004.

REFERENCES

Ahn, Y. C., Cho, J. M., Cha, S. R., Lee, J. K., Park, Y. O., Kim, S. D. and Lee, S. H., "Physical, chemical and electrical analysis of dust generated from cement plants for dust removal with an electrostatic precipitator," *Korean J. Chem. Eng.*, **21**, 182 (2004).

Chang, J. S., Brocilo, D., Urashima, K., Dekowski, J., Podlinski, J., Mizeraczyk, J. and Touchard, G., *On-set of EHD turbulence for cylinder in cross flow under corona discharges*, Proceedings of the 5th International EHD workshop, 30-31 August, Poitiers, France, 26-31 (2004).

Chang, J. S., McLinden, C. A., Berezin, A. A., Looy, P. C. and Kaneda, T., "Modelling of quadrupole cold precharger dust particle charging characteristics," *Report of School of Engineering*, Tokyo Denki University, **44**, 1 (1996).

Chang, J. S., Pontiga, F., Kwan, A. L. C. and Kaneda, T., "Modelling of coaxial wire-pipe negative glow corona discharges with and without external magnetic fields," *Report of School of Engineering*, Tokyo Denki University, **45**, 11 (1997).

Choi, B. S. and Fletcher, C. A. J., "Computation of particle transport in an electrostatic precipitator," *Journal of Electrostatics*, **40**(41), 413 (1997).

IEEE-DEIS-EHD Technical Committee, "Recommended international standard for dimensionless parameters used in electrohydrodynamics," *IEEE Transactions on Dielectrics and Electrical Insulation*, **10**(1), 3-6, February (2003).

Launder, B. E. and Spalding, D. B., "The numerical computation of turbulent flows," *Computer Methods in Applied Mech. and Eng.*, **3**, 269 (1974).

Liang, W. J. and Lin, T. H., "The characteristics of lonic wind and its effect on electrostatic precipitators," *Aerosal Sci. Tech.*, **20**, 330 (1994).

Michel, F., *New Features of MIGAL solver*, in Proceedings of the 9th International PHOENICS User Conference, Moscow, Russia, 23-27 (2002).

Mizeraczyk, J., Kocik, M., Dekowski, J., Dors, M., Podliński, J., Ohkubo, T., Kanazawa, S. and Kawasaki, T., "Measurements of the velocity

field of the flue gas flow in an electrostatic precipitator model using PIV method," *Journal of Electrostatics*, **51**(52), 272 (2001).

Monson, D. J., Seegmiller, H. L., McConnaughey, P. K. and Chen, Y. S., *Comparison of experimental with calculations using curvature-corrected zero and two-equation turbulence models for a two-dimension U-duct*, AIAA-90-1484 (1990).

Park, H. S. and Park, Y. O., "Simulation of particle deposition on filter fiber in an external electric field," *Korean J. Chem. Eng.*, **22**, 303 (2005).

Park, S. J. and Kim, S. S., "Electrohydrodynamic flow and particle transport mechanism in electrostatic precipitators with cavity walls," *Aerosol Science and Technology*, **33**, 205 (2000).

Patel, V. C., Rodi, W. and Scheurer, G., "Turbulence models for near-wall and low-Reynolds-number flows: A review," *AIAA J.*, **23**(9), 1308 (1985).

Riehle, C. and Löffler, F., "Grade efficiency and eddy diffusivity models," *J. Electrostatics*, **34**, 401 (1995).

Schemid, H. J., Stolz, S. and Buggisch, H., "On the modelling of the electro-hydrodynamic flow field in electrostatic precipitators flow," *Turbulence and Combustion*, **68**, 63 (2002).

Yakhot, V. and Orszag, S. A., "Renormalization group analysis of turbulence," *J. Sci. Comput.*, **1**, 3 (1986).

Yamamoto, T. and Velkoff, H. R., "Electrohydrodynamics in an electrostatic precipitator," *J. Fluid Mech.*, **108**, 1 (1981).

Yap, C., *Turbulent heat and momentum transfer in recirculating and impinging flows*, PhD Thesis, Faculty of Technology, University of Manchester (1987).